Guanine, a high-capacity and rapid-turnover nitrogen reserve in microalgal cells

Peter Mojzeš[a,b], Lu Gao[b,c], Tatiana Ismagulova[d], Jana Pilátová[e], Šárka Moudříková[a], Olga Gorelova[d], Alexei Solovchenko[d,f], Ladislav Nedbal[b,1], and Anya Salih[g,h]

[a]Institute of Physics, Faculty of Mathematics and Physics, Charles University, CZ-12116 Prague 2, Czech Republic; [b]Institute of Bio- and Geosciences/Plant Sciences (IBG-2), Forschungszentrum Jülich, D-52428 Jülich, Germany; [c]Faculty of Mathematics and Natural Sciences, Heinrich Heine University, D-40225 Düsseldorf, Germany; [d]Faculty of Biology, Moscow State University, Leninskie Gori 1/12, 119234, GSP-1, Moscow, Russia; [e]Department of Experimental Plant Biology, Faculty of Science, Charles University, CZ-12844 Prague 2, Czech Republic; [f]Faculty of Geography and Natural Sciences, Pskov State University, 180000 Pskov, Russia; [g]Antares Fluoresci Research, Dangar Island, NSW 1797, Australia; and [h]Confocal Bioimaging Facility, Western Sydney University, NSW 1797, Australia

Edited by Donald R. Ort, University of Illinois at Urbana–Champaign, Urbana, IL, and approved November 4, 2020 (received for review May 3, 2020)

Nitrogen (N) is an essential macronutrient for microalgae, influencing their productivity, composition, and growth dynamics. Despite the dramatic consequences of N starvation, many free-living and endosymbiotic microalgae thrive in N-poor and N-fluctuating environments, giving rise to questions about the existence and nature of their long-term N reserves. Our understanding of these processes requires a unequivocal identification of the N reserves in microalgal cells as well as their turnover kinetics and subcellular localization. Herein, we identified crystalline guanine as the enigmatic large-capacity and rapid-turnover N reserve of microalgae. The identification was unambiguously supported by confocal Raman, fluorescence, and analytical transmission electron microscopies as well as stable isotope labeling. We discovered that the storing capacity for crystalline guanine by the marine dinoflagellate *Amphidinium carterae* was sufficient to support N requirements for several new generations. We determined that N reserves were rapidly accumulated from guanine available in the environment as well as biosynthesized from various N-containing nutrients. Storage of exogenic N in the form of crystalline guanine was found broadly distributed across taxonomically distant groups of microalgae from diverse habitats, from freshwater and marine free-living forms to endosymbiotic microalgae of reef-building corals (*Acropora millepora*, *Euphyllia paraancora*). We propose that crystalline guanine is the elusive N depot that mitigates the negative consequences of episodic N shortage. Guanine ($C_5H_5N_5O$) may act similarly to cyanophycin ($C_{10}H_{19}N_5O_5$) granules in cyanobacteria. Considering the phytoplankton nitrogen pool size and dynamics, guanine is proposed to be an important storage form participating in the global N cycle.

nitrogen cycle | nutrient storage | phytoplankton | guanine | coral

Planktonic algae represent an essential driver of the global carbon cycle, which may be constrained by low or fluctuating nitrogen (N) availability (1–3). At another extreme, high levels of bioavailable N, often from anthropogenic sources, may result in harmful algal blooms (4) or deterioration of coral reefs (5). The highly optimized nutrient interactions with symbiotic algae are also essential for reef corals that thrive in nutrient-poor waters and paradoxically form among the most productive and diverse ecosystems. Both high and low N availability may perturb the stability of individual organisms or entire ecosystems especially when not in proportion to other biogenic elements, such as phosphorus (6).

N shortages trigger extensive changes in algal metabolism (7), including cessation of cell division, reduction of photosynthesis, and accumulation of C- and energy-rich N-free compounds. Unlike cyanobacteria, eukaryotic microalgae do not possess N-rich cyanophycin to manage N deficiency (8, 9). N-deprived microalgae mobilize intracellular inorganic N; low-molecular organic N compounds, such as polyamines, amino acids, and chlorophyll (7); and polymeric N compounds, such as proteins and nucleic acids (10). However, none of these reserves may be sufficient to bridge long periods of N starvation. Thus, a pool capable of storing large amounts of N during periods of abundance and ensuring survival and growth of algae during deficiency remains to be identified.

Among candidate N storage pools in microalgae, crystalline inclusions were considered, although later, alternative roles, such as processing of metabolic wastes (11) and light modulation (12) were also suggested. The chemical identity of crystals from the free-living marine dinoflagellate *Gonyaulax polyedra* was proposed to be guanine (13). Other crystalline inclusions hypothesized of being guanine were also observed in symbiotic dinoflagellates of an anemone *Aiptasia* sp. (14), but their chemical nature was not experimentally confirmed (11, 14). Other earlier studies suggested the inclusions were calcium oxalate (15, 16) making the N-storage function of the inclusions unlikely. Subsequent analysis of symbiotic dinoflagellate extracts from *Aiptasia* sp. identified them as crystalline uric acid (17). This identification has since been adopted for microalgal inclusions in many recent publications (18–21).

In contrast with this proposed identity (17–21) and consistent with earlier studies (13, 14), recent direct in situ analyses identified inclusions as guanine in several marine dinoflagellates (12, 22), a freshwater chlorophyte and a eustigmatophyte (23). Guanine, similar to other purines, has the potential to serve as a large-capacity N pool, but this function has never been previously confirmed, nor was its in situ chemical identity explored in diverse algal species. Guanine is widespread and, thus, widely available in nature. It is an essential component of DNA and RNA, one of the end products of

Significance

Vast areas of the oceans are N limited, and how microalgae can flourish in these N-poor waters is still not known. Furthermore, mechanisms and sites of N uptake and storage have not been fully determined. We show that crystalline guanine ($C_5H_5N_5O$) is an important N storage form for phytoplankton and for symbiotic dinoflagellates of corals. The widespread occurrence of guanine reserves among taxonomically distant microalgal species suggests an early evolutionary origin of its function as N storage. Crystalline guanine appears to be a multifunctional biochemical with an important role in the N cycle that remains to be elucidated. In particular, a better knowledge of N-storage metabolism is necessary to understand the impact of eutrophication on coral-symbiont interaction.

Author contributions: P.M., A.So., and L.N. designed research; P.M., L.G., T.I., J.P., O.G., A.So., and A.Sa. performed research; P.M., L.G., T.I., O.G., A.So., L.N., and A.Sa. analyzed data; and P.M., L.G., A.So., L.N., and A.Sa. wrote the paper.

The authors declare no competing interest.

This article is a PNAS Direct Submission.

[1]To whom correspondence may be addressed. Email: l.nedbal@fz-juelich.de.

This article contains supporting information online at https://www.pnas.org/lookup/suppl/doi:10.1073/pnas.2005460117/-/DCSupplemental.

First published December 8, 2020.

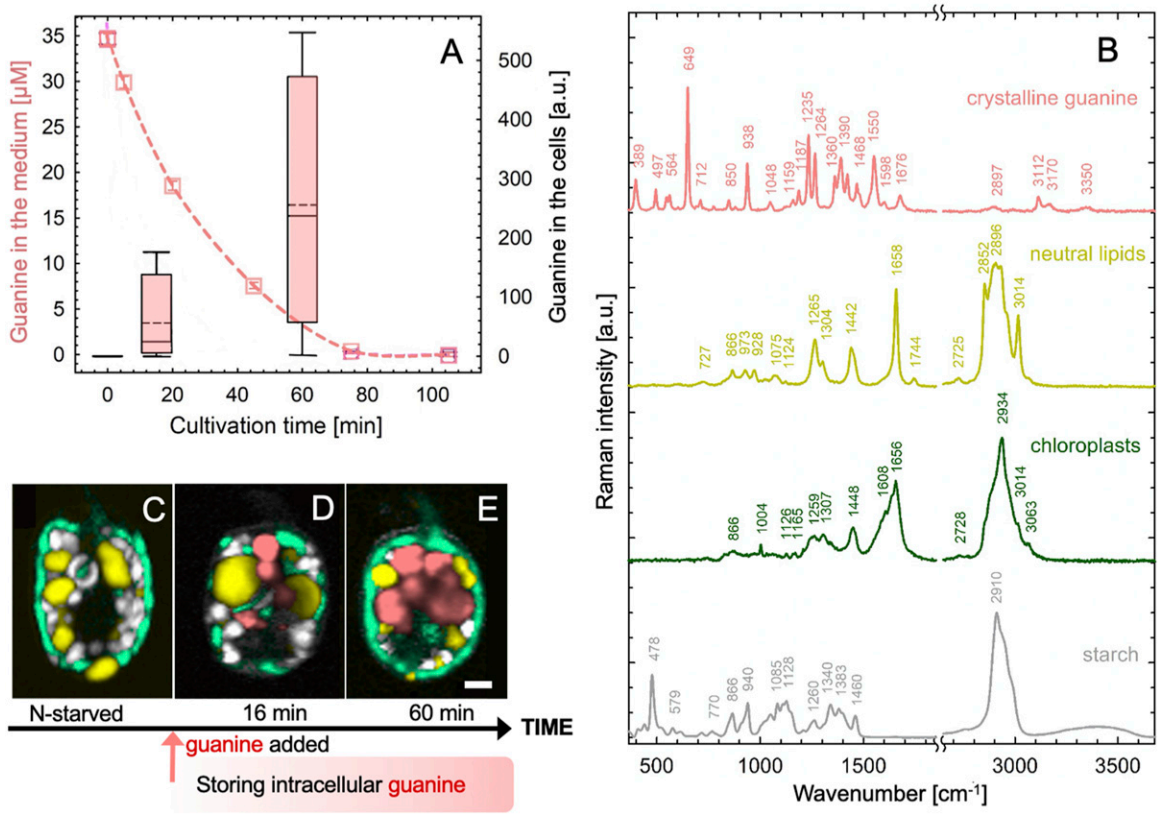

Fig. 1. Rapid uptake of guanine by N-starved *A. carterae* led to the accumulation of intracellular guanine inclusions. Cells were suspended in a saturated solution of guanine (~35 μM at 20 °C) in N-deficient f/2 medium at a density of $1.7 \pm 0.3 \times 10^5$ cells·mL^{-1}. The dashed line in *A* shows the declining concentration of guanine in the medium as measured by ultraviolet absorption (*SI Appendix*, section II.1.B). The simultaneous accumulation of guanine in the cells was assessed using Raman microscopy (*SI Appendix*, section II.1.C) and is shown in the boxplot. Raman spectra in *B* were used to generate the Raman maps in *C–E* that represent: (*C*) a typical cell after 2 wk without a N source and (*D* and *E*) cells during progressive guanine accumulation. Color legend: guanine (pink), lipids (yellow), chloroplast (green), and starch (white/gray). (Scale bar, 2 μm.) Raman maps showing separate cellular constituents in *C–E* are constructed as described in *SI Appendix*, section I.1 and presented in *SI Appendix*, Fig. S1.

nucleic acid degradation in some organisms, and utilized by some for functional purposes, such as light scattering by silvery scales of fish and bio-optical systems of many invertebrates (reviewed in ref. 24). It is widely available from decomposing fish tissues and scales, from ciliates and some phytoplankton, barnacles, and other aquatic organisms and forms part of suspended and dissolved organic N pools in the ocean. Along with other purines, guanine can serve as a N source for algae (reviewed in ref. 1). We propose that crystalline guanine and other purines (17) play a more prominent role in the N cycle than recognized to date.

To test this hypothesis, we used the unique potential of Raman microscopy and analytical transmission electron microscopy (TEM) and identified the chemical nature and the dynamics of microalgal crystal inclusions. We confirm the occurrence of crystalline guanine in free-living and symbiotic dinoflagellates and other diverse microalgal species. Our research demonstrated widespread occurrence, large N-storage capacity, and prominent dynamics of guanine in the form of crystalline inclusions in microalgae.

Results

Fast Kinetics of Uptake and Large Storage Capacity of Intracellular Guanine Inclusions in *Amphidinium carterae*. We first characterized the uptake of guanine by the widespread potentially toxic marine dinoflagellate *A. carterae*. Details of cultivation are provided in *SI Appendix*, section II.1A. Cells were kept in N-free medium (*SI Appendix*, section II.1.Aa.) for approximately 2 wk before resuspension in a saturated solution of guanine (*SI Appendix*, section II.1.Ab.). We recorded a rapid uptake rate of dissolved guanine from the medium (dashed line, Fig. 1*A*) and its concurrent accumulation in cells (box plot, Fig. 1*A*). Dynamics and localization of guanine inclusions inside cells (in pink, Fig. 1 *C* and *D*) on the background of other cellular components was identified by the spectral signature of Raman confocal microscopy (Fig. 1*B*) (23). The rapid accumulation of the optically active guanine crystals was also documented via polarization microscopy (*SI Appendix*, section II.1.D. and Movie S1).

The dependence of uptake kinetics of dissolved guanine (Fig. 2 and *SI Appendix*, section I.2.) on cell density displayed an initial linear uptake phase (solid lines, the coefficient of determination RSQR ≥ 0.995) and its interpolation yielded an initial cellular uptake rate of 16 ± 4 fg (guanine)·s^{-1}·cell^{-1}, i.e., $6.3 \pm 1.5 \times 10^7$ molecules·s^{-1}·cell^{-1}.* Uptake kinetics (Fig. 2) were used to quantify intracellular guanine accumulation inside cells (*SI Appendix*, Fig. S2*A*) resulting in a maximum storage capacity of 143 ± 37 pg of crystalline guanine cell^{-1}, that corresponded to 68 ± 17 pg (nitrogen)·cell^{-1}. Details of these calculations are provided in *SI Appendix*, section I.2. The N pool created by starvation and refeeding was significantly larger than 17–44 pg (nitrogen)·cell^{-1} that was previously suggested to be the total N content in *A. carterae* under stationary conditions (25). Guanine storage pools may, thus, ameliorate N deficiency that occurs sporadically in a fluctuating environment.

*Numbers following the ± sign represent, in this work, standard deviation.

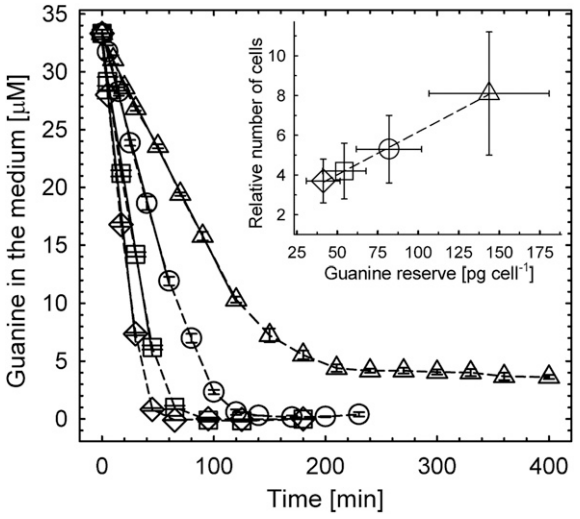

Fig. 2. Uptake of dissolved guanine from the medium by N-starved *A. carterae* and the number of generations supported by accumulated reserves (inset). The rate of guanine disappearance from the medium decreased with reduced cell density (±SD): from (122 ± 31) (◇) to (93 ± 23) (□), to (61 ± 15) (○), and to (31 ± 8) (△) × 10^3 cells·mL^{-1}. The most dilute culture (△) reduced guanine concentration in the medium from 35 to ~4 μM, revealing the maximum storage capacity of cells of 143 ± 37 (SD) pg of crystalline guanine cell^{-1}. *Inset* shows the correlation between the number of cells grown on guanine reserve and the reserve size. Details of calculations for this figure are described in *SI Appendix*, section I.2 and Fig. S2.

Cells with new guanine reserves can, after a short lag period, resume normal cell division and growth. The exponential growth phase halted only after the reserves were once again exhausted (*SI Appendix*, Fig. S2*B*). The number of cells that grew on these reserves was a linear function of the initially available guanine (inset in Fig. 2). The number of cells that accumulated maximum N storage (△) increased 8.1 ± 3.1 times without N addition.

The resolution of the in situ localization of guanine crystals in *A. carterae* (Fig. 1) was increased via ultrastructural TEM imaging (Fig. 3 and *SI Appendix*, section II.1.E.) (26, 27). The solubility of guanine is known to be extremely low, and pieces of undissolved crystalline material (Fig. 3*A*, three white arrows) were confirmed via EDX (*SI Appendix*, section II.1.F.) to correspond to the elemental composition of a N-rich compound, likely to be guanine (Fig. 3*D*). *A. carterae* has a special organelle, the pusule, which is connected to the flagellar channel (28, 29). We found large globules in pusules (Fig. 3 *B* and *C*) and small crystals in vacuoles that consistently displayed typical EDX point spectra of guanine crystals (Fig. 3 *E* and *F*). Our results were inconclusive with respect to whether the guanine particles had been taken up into the pusules by phagocytosis (30) and/or via an active transport of guanine molecules dissolved in the medium from the added crystals. Guanine globules in pusules and vacuoles had irregular shapes, but the comparison of Raman spectra (Fig. 1*B*) with those in refs. 12, 31 confirmed that the molecules were organized in a regular anhydrous crystal structure. We hypothesized that algae may take up guanine microcrystals and, possibly, guanine-rich marine particulate fish debris via endocytosis or via the pusule (*SI Appendix*, sections I.3 and II.1.Ac and Fig. S3).

Uptake of Solid Guanine by *A. carterae* Involves Crystal Decomposition and Recrystallization. Guanine microparticles or guanine-rich debris might be taken up by dinoflagellates and directly deposited inside their cells without first dissolving or changing the original crystalline structure, similar to an engulfing mechanism proposed for algal feeding on bacteria (32). In an alternative scenario, the engulfed particles may be first dissolved within pusules or vacuoles into individual molecules. Globules of guanine may then be assembled at target intracellular locations by new crystallization (Figs. 1 and 3). Guanine crystals may also be dissolved extracellularly,

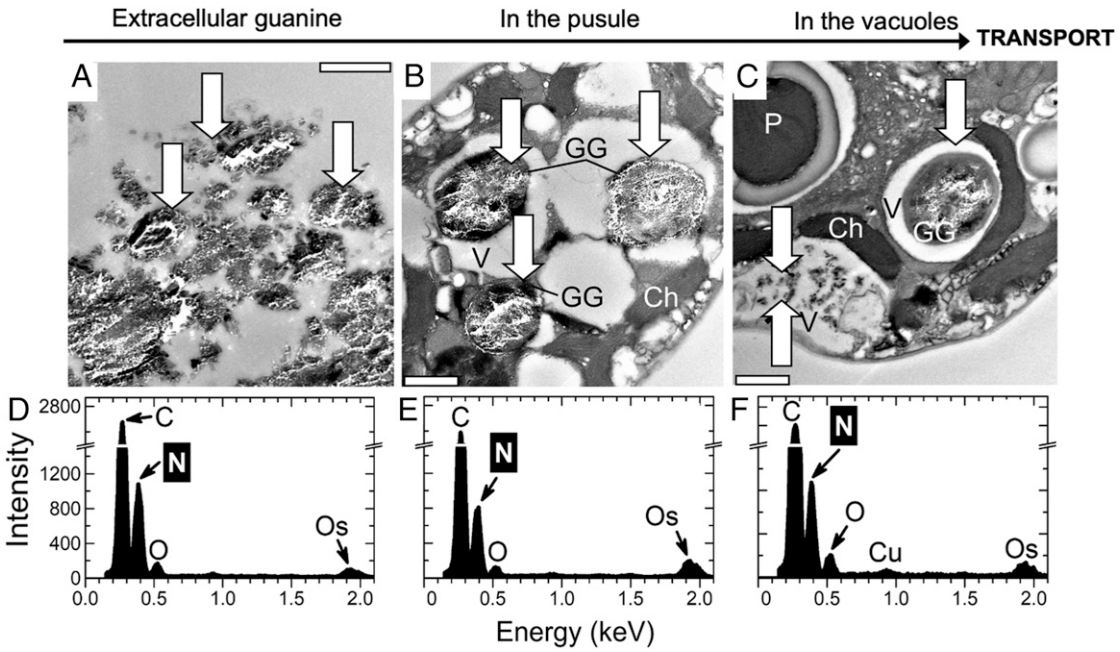

Fig. 3. TEM of semithin sections (*A–C*) and energy-dispersive X-ray spectroscopy (EDX) (*D–F*) analysis of *A. carterae* 6 h after refeeding N-starved cultures with guanine. Typical EDX point spectra of guanine crystals (*D–F*) indicating a high N content were obtained in the scanning TEM (STEM) mode from semithin cell sections. Arrows point to guanine particles outside (*A*) and inside cells (*B* and *C*). (Scale bars, 1 μm.) Ch, chloroplast; GG, globules with microcrystalline guanine; P, pyrenoid; V, vacuole.

subsequently taken up via active constitutive transport through their cell walls and reassembled into crystalline structures inside the cells.

Raman microscopy offers a unique opportunity to discriminate between the uptake mechanisms using the spectral contrast between fully (d_5) and partially (d_1) deuterated guanine (Fig. 4 and *SI Appendix*, sections I.3 and II.2.A and Fig. S7). The conversion of d_5-guanine to d_1-guanine requires that the molecules are directly exposed to an aqueous environment so that the four deuterium atoms bound to N can be exchanged by hydrogen from water, leaving only deuterium bound to C8 (33). Thus, if the guanine particle remained in its original crystalline form during the uptake by a cell, the N-D groups of d_5-guanine would have been protected from isotope exchange. Confirming this, a grain of guanine crystal outside of a cell (Fig. 4*B*) was found to remain in the d_5-guanine form (dark blue, white arrow).

The Raman spectra proved that the new reserves of intracellular guanine that appeared inside the N-starved *A. carterae* were in the d_1 form (Fig. 4, magenta). Only 30 min after the crystalline d_5-guanine was added to the cell suspension, both the d_5-guanine grain (dark blue, white arrow) outside the cell and the transformed d_1-guanine globules inside the cells (magenta) were captured simultaneously in Fig. 4 *A* and *B*. Crystalline d_1-guanine was also found in the cells 5–12 h after feeding (Fig. 4 *D* and *F*). The large guanine globules were preferentially located at the cell center 5 h after N feeding (Fig. 4 *C* and *D*), and, subsequently, some in the form of smaller particles moved toward the cell periphery (Figs. 4 *E* and *F* and 3*C*).

Our analyses suggest that the guanine microcrystals were dissolved outside cells and taken up as individual molecules. Alternately, if they were engulfed as intact microcrystals, they were then dissolved intracellularly before reassembling into new crystals. In either case, the original crystalline structure was released, deuterium atoms bound to N in the d_5-form were exchanged for hydrogen from water, and the d_1-guanine molecules were reassembled into much larger inclusions in the vacuoles and/or pusules (Figs. 3 and 4).

Guanine Crystals Are Biosynthesized in *A. carterae* de Novo from Diverse Exogenic N Sources. Raman spectroscopy can also easily distinguish between ^{14}N- and ^{15}N-guanine (*SI Appendix*, sections I.3 and II.2.B and Fig. S8), thus, making it useful for determining the source of N. Feeding N-starved *A. carterae* with ^{15}N-guanine, ^{15}N-nitrate, ^{15}N-ammonium (*Top* in Fig. 5), or ^{15}N-urea (*SI Appendix*, Fig. S10) restored the culture's growth and, regardless of the N source,

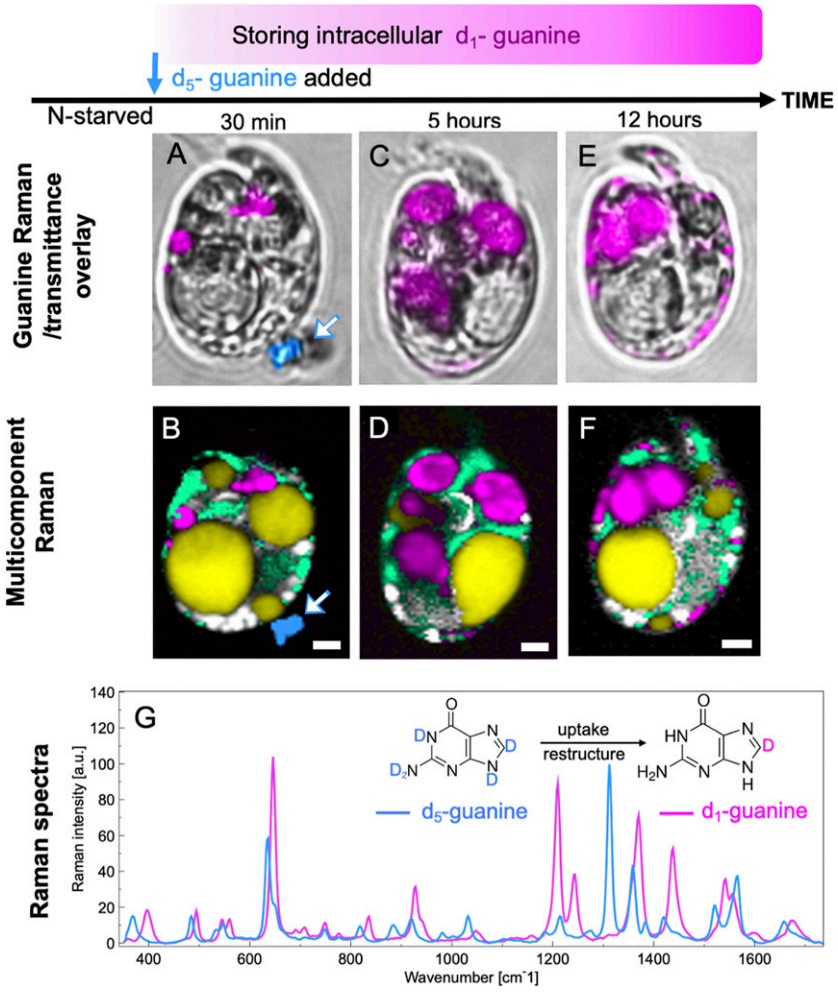

Fig. 4. Uptake of guanine includes exchange of deuterium for hydrogen atoms. Bright-field images overlaid by guanine (*A*, *C*, and *E*) and multicomponent Raman maps (*B*, *D*, and *F*) of N-starved *A. carterae* after the addition of solid crystalline fully deuterated d_5-guanine to N-depleted medium. Images collected 30 min (*A* and *B*), 5 h (*C* and *D*), and 12 h (*E* and *F*) after d_5-guanine addition. Data for d_5-guanine and partially deuterated d_1-guanine are presented in blue and magenta, respectively, in both the Raman spectrum and the images. *G* shows their respective Raman spectra. Other colors: yellow, neutral lipids; green, chloroplasts; white/gray, starch. (Scale bars [*A*–*F*], 2 μm.) More spectra of isotopically labeled guanine are shown in *SI Appendix*, Fig. S7. Raman maps showing separate components from data represented in *B*, *D*, and *F* are provided in *SI Appendix*, Fig. S9.

considerable amounts of crystalline ^{15}N-guanine appeared inside the cells during the *lag* phase that lasted ~24 h (Fig. 5, *Bottom*). On feeding *A. carterae* with nitrate, ammonium, or urea, no crystalline inclusions of other purines were observed. The accumulated or biosynthesized guanine crystals were later used to support growth until their complete disappearance in the new stationary phase. Regardless of the chemical identity of the N source, the total amount of N needed to produce a new *A. carterae* cell, estimated from the data in Fig. 5, was 14 ± 2 pg (N)·cell^{-1}. The calculation procedure was the same as in *SI Appendix*, section I.2. This amount corresponded theoretically to 30 ± 4 pg (guanine)·cell^{-1} of the presumed reserve, which was close to 23 ± 4 pg (guanine)·cell^{-1} obtained from the data presented in the graph inset in Fig. 2.

Interestingly, the intracellular guanine reserves generated by the assimilation of nitrate (middle graph in Fig. 5), ammonium, or urea were detected largely at the periphery of cells close to the chloroplasts (Fig. 6). This was in agreement with the earlier results obtained for nitrate (12). In contrast, the rapidly accumulated guanine was first located centrally in large globules (Fig. 4 *C* and *D* and *SI Appendix*, Fig. S11), which were later partially fragmented and moved to the cell periphery (Fig. 4*E*). This result obtained by Raman microscopy was confirmed with significantly higher spatial resolution by the combination of TEM and EDX methods (Figs. 3 and 6). We tentatively propose that the aforementioned differences in localization and storage dynamics indicate differences in transport and biochemical pathways following guanine biosynthesis from nitrate, ammonium, and urea compared with the direct uptake of guanine.

In Situ Chemical Identification of Inclusions in Algal Species of Diverse Taxonomical Classification and from Diverse Habitats. The chemical identity of inclusions in 14 microalgal species listed in Table 1 was examined by Raman microscopy as described in *SI Appendix*, section II.1.C. The selected species (*SI Appendix*, sections I.4. and II.3 for cultivation conditions) represent contrasting habitats, such as oligotrophic to mesotrophic marine species including both free-living (*A. carterae* and *Microchloropsis gaditana*) and coral endosymbiotic algae (*Chromera velia* and *Symbiodiniaceae*), oligotrophic to eutrophic freshwater (*Synura petersenii* and *Haematococcus pluvialis*, respectively), extremophilic/acidophilic (*Dunaliella acidophila*), terrestrial (*Lobosphaera incisa, Vischeria* sp., and *Klebsormidium flaccidum*), and algae from artificial anthropogenic environments (*Vacuoliviride crystalliferum* and *K. flaccidum*), their distribution ranging from tropical/subtropical regions (*A. carterae*, *C. velia*, and *Symbiodiniaceae*) and temperate zones (*Vischeria* sp.) to the cosmopolitan species extending to the Arctic (*K. flaccidum*). Some of the tested species were established model organisms (*Chlamydomonas reinhardtii* and *Microchloropsis gaditana*), others were important production species in algal biotechnology (*M. gaditana*, *D. acidophila*, *H. pluvialis*, and *L. incisa*). The diverse phylogeny among the selected species is shown in Table 1. Spectral signatures of inclusions found in the selected algal species were compared with the spectra of multiple purines (*SI Appendix*, Fig. S4) and with calcium oxalate and calcite (*SI Appendix*, Fig. S6). Guanine inclusions were found in 13 out of 14 tested species cultivated in commonly used media (*SI Appendix*, section II.3). Only one of the tested species *K. flaccidum* was found to contain uric acid in its inclusions. This identification was completed in situ, thus, eliminating the potential artifacts caused by extraction and chemical analyses. Differences between Raman spectral signatures of guanine and uric acid are large (*SI Appendix*, Fig. S4), enabling accurate discrimination needed in light of alternatives proposed in recent literature (12, 17, 23). We cannot rule out, however, that under specific cultivation conditions, stress factors, or feeding by other organic nutrients, crystalline inclusions of other purines may not be present. Furthermore, the abundance of guanine inclusions depended not only on the availability of N nutrients (Fig. 1 *C–E*), but also on cultivation factors, such as CO_2 availability for *Desmodesmus quadricauda* (23) or on the cell cycle phase in *C. reinhardtii* (*SI Appendix*, section I.4 and Fig. S12). We also cannot exclude possible transformation of different purine forms with some perhaps occurring transiently or even simultaneously. Nevertheless, our experiments reliably confirm that guanine is the dominant N-storage form in the investigated microalgal species, and uric acid is found only in *K. flaccidum*, a single representative of the Streptophyta lineage. However, many more species of this lineage must be tested in the future to conclude that the Streptophyta lineage deviates from other taxonomical groups.

Coral Symbiotic Microalgae Accumulate and Store Guanine. Of particular interest in relation to guanine cell storage are the photosynthetic *Symbiodiniaceae* dinoflagellates (zooxanthellae) that live in mutualistic symbiosis with reef-building corals. The finely tuned exchange of nutrients between the coral host and the symbionts forms the foundation of healthy coral reef ecosystems (5, 21, 34, 35). However, much remains poorly understood regarding the mechanisms of nutrient uptake and storage that allow corals to

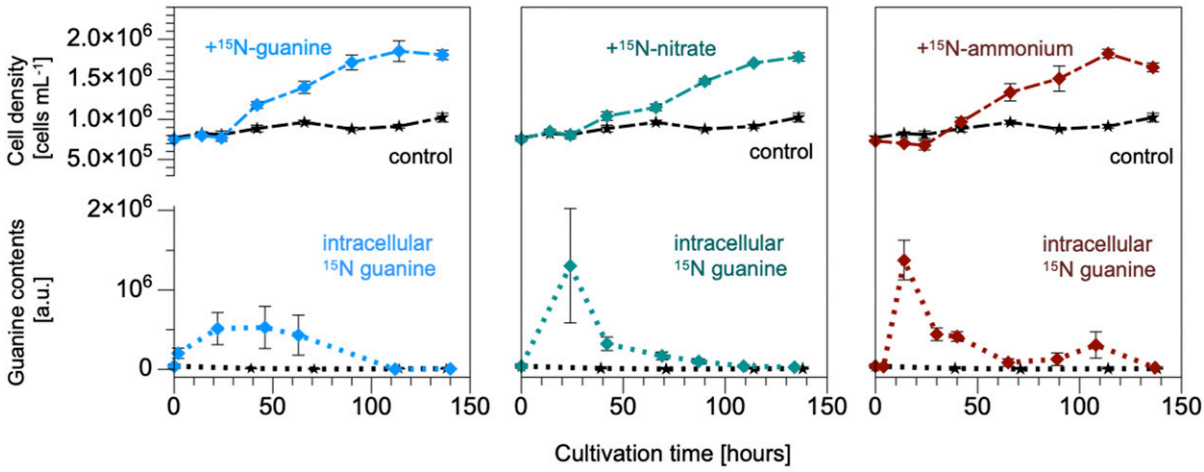

Fig. 5. N in guanine inclusions originated directly from the supplied guanine, nitrate, and ammonium. *A. carterae* cell density stagnated in controls without N feeding (black lines) and divided after addition of ^{15}N-labeled guanine, nitrate, and ammonium (all at 0.882-mM N). Intracellular crystalline guanine per cell is shown in the bottom graphs representing Raman measurements (n = 5–12 cells). The corresponding graph representing uptake of urea is shown in *SI Appendix*, Fig. S10.

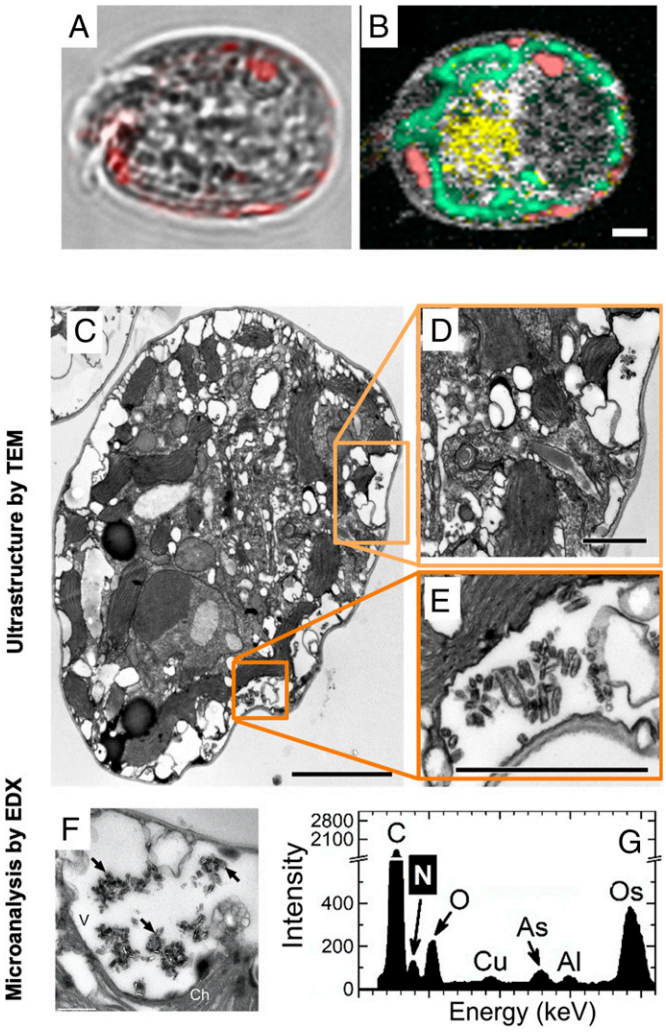

Fig. 6. Localization of guanine inclusions in *A. carterae* fed by nitrate by TEM. Bright-field images overlaid by guanine (pink) (*A*) and multicomponent Raman maps (*B*) of *A. carterae* cells 24 h after refeeding N-starved cells with nitrate. False color coding is the same as that in Fig. 1. (Scale bar, 2 μm.) TEM of ultrathin (*C*–*E*) and semithin (*F*) sections as well as EDX (*G*); (*F* and *G*) analysis of *A. carterae* cells and surrounding cells 26 h after refeeding N-starved cultures with nitrate. Typical EDX point spectra of guanine crystals (*G*) indicating high N content were obtained in the STEM mode from semithin cell sections. Arrows point to guanine crystals. (Scale bars, 2.5 [*C*], 1 [*D* and *E*], and 0.5 μm [*F*]. Ch, chloroplast; V, vacuole.)

survive in the N-poor waters of tropical seas or cope with pulses of excessive nutrients due to upwelling or rainfall (5, 34, 35).

We demonstrated in this study that the numerous crystalline inclusions of endosymbiotic *Symbiodiniaceae* consist of guanine and that the external guanine is rapidly assimilated into the symbionts (Fig. 7 and *SI Appendix*, section I.5.). According to Raman microscopy (*SI Appendix*, Fig. S14), *Symbiodiniaceae* cells in the tissue of the scleractinian coral *Euphyllia paraancora* (*SI Appendix*, sections I.5 and II.4.A) exhibited similar guanine pool dynamics (Fig. 7 *A*–*C*) as the free-living dinoflagellate *A. carterae* (Figs. 1–4). *Symbiodiniaceae* from corals grown under optimal conditions always contained large guanine reserves (Fig. 7*A*). After 4 mo of N starvation of corals, guanine reserves were found depleted (Fig. 7*B*), the polyps shrank and became partially bleached. Upon refeeding with ^{15}N-$NaNO_3$, the newly synthesized ^{15}N-guanine inclusions appeared within 24 h inside *Symbiodiniaceae* cells (Fig. 7*C* and *SI Appendix*, Fig. S14).

The dynamic uptake of guanine was further confirmed in the *Symbiodiniaceae*-hosting coral *Acropora millepora*, which is widespread on the GBR, Australia, by using a combination of confocal fluorescence and reflection imaging (Fig. 7 *D*–*F* and *SI Appendix*, sections I.6 and II.1.C). *A. millepora* that was freshly collected from the GBR (Marine Parks Authority Permit G17/39943.1 to A.Sa., method in *SI Appendix*, section II.4.B) contained varying quantities of guanine crystals scattered peripherally among chloroplast lobes (Fig. 7*D* and *SI Appendix*, Fig. S15). Prolonged N starvation resulted in complete depletion of the guanine reserves (Fig. 7*E*). When the N-starved *Symbiodiniaceae* cells isolated from *A. millepora* were fed by a small amount of guanine powder added directly to the medium, the highly reflective guanine particles that were first visualized outside *Symbiodiniaceae* cells, began to accumulate inside cells after ∼1 h (Fig. 7*F*). A similar direct uptake of guanine was observed in *Symbiodiniaceae* extracted from the zoanthid *Zoanthus* sp. (*SI Appendix*, Fig. S16, *Bottom*) and in free-living *A. carterae* (in *SI Appendix*, Fig. S16, *Top* and Movie S1).

The same dynamics of appearance and disappearance of guanine inclusions were observed for *Symbiodiniaceae* of four other cnidarian species—the anemone *Aiptasia* sp., corallimorpharian, *Rhodactis indosinensis*, leather soft coral, *Sinularia asterolobata*, and *Zoanthus* sp., cultivated in an experimental aquarium (method in *SI Appendix*, section II.4.A). This is an in situ identification of the crystalline guanine within the intact symbiotic zooxanthellae from multiple anthozoan species.

Discussion

Guanine ($C_5H_5N_5O$) holds 1.9-fold higher amounts of N per unit molecular weight than a monomer of N-storing cyanophycin ($C_{10}H_{19}N_5O_5$), known to be the long-term N reserve in cyanobacteria. The ratio is even higher when the hydration of cyanophycin is considered. As it is uncharged and almost insoluble at physiological pH, crystalline guanine is less metabolically active than various ionic N-containing compounds, enabling its accumulation in large quantities and its long-term storage inside cells without the risk of metabolic disorder. In comparison with other purines, guanine is one order of magnitude less soluble than uric acid or xanthine and two orders of magnitude less soluble than adenine or hypoxanthine. It is also more chemically stable than uric acid (1). Yet guanine can be easily mobilized from the solid state by changing pH of its aqueous environment. Although almost insoluble at neutral pH, its solubility in water increases greatly at acidic or basic pH (31). Algal metabolic activity is highly pH dependent: photosynthesis increases the pH during the day, respiration decreases it at night, and a variety of cellular pH controls alter it in response to environment and stress (36). Thus, it is possible that guanine's solubility is under cellular pH control, facilitating its transport and assimilation. In coral-algal symbiosis, pH influences the flow of N between the host and its symbionts (35) and guanine's pH solubility dependence may make it a perfect metabolic N-storage molecule. Importantly, our finding that the size of the guanine reserve in planktonic microalgae can be much higher than the N amount required for cell reproduction indicates that it is a major N pool of global importance, being proportional to the phytoplankton biomass and matching its contributions to global carbon and N cycles (2, 37).

Biogenic guanine forms a highly compact crystal structure, namely, the β-form of the anhydrous monoclinic polymorph, consisting of vertically stacked planes of hydrogen-bonded molecules (12, 38). This crystal structure explains its unique optical properties, including birefringence and an extremely high index of refraction, leading to high light scattering as recorded in our confocal reflective imaging analysis. Consequently, guanine's storage function does not exclude other possible functions, e.g., light scattering in microalgae to enhance the efficiency of photosynthesis, photoprotection from UV radiation, or the formation of photonic mirrors (12, 38).

Table 1. Microcrystalline purines identified by Raman microscopy in various algal strains

Species	Habitat	Phylogeny	Purine
Symbiodiniaceae	E-S	Alveolata–Dinoflagellata	Guanine
Amphidinium carterae	S	Alveolata–Dinoflagellata	Guanine
Chromera velia	S	Alveolata–Chromerida	Guanine
Microchloropsis gaditana	S	Stramenopiles–Eustigmatophyceae	Guanine
Vacuoliviridecrystalliferum	U	Stramenopiles–Eustigmatophyceae	Guanine
Vischeria sp.	T	Stramenopiles–Eustigmatophyceae	Guanine
Trachydiscus minutus	F	Stramenopiles–Eustigmatophyceae	Guanine
Synura petersenii	F	Stramenopiles–Chrysophyceae	Guanine
Lobosphaera incisa	F, T	Archaeplastida–Chlorophyta–Trebouxiophyceae	Guanine
Desmodesmus quadricauda	F	Archaeplastida–Chlorophyta–Chlorophyceae	Guanine
Chlamydomonas reinhardtii	F	Archaeplastida–Chlorophyta–Chlorophyceae	Guanine
Dunaliella acidophila	Acid	Archaeplastida–Chlorophyta–Chlorophyceae	Guanine
Haematococcus pluvialis	F	Archaeplastida–Chlorophyta–Chlorophyceae	Guanine
Klebsormidium flaccidum	T	Archaeplastida–Streptophyta–Klebsormidiophyceae	Uric acid

The screened species represent diverse habitats: Acid, acidophilic; E, endosymbiotic; F, freshwater; S, marine; T, terrestrial/aerophytic; U, unspecified. The origins of the examined species as well as cultivation approach are described in *SI Appendix*, sections I.4 and II.3.

N is limiting to phytoplankton primary productivity in many marine ecosystems and is often associated with sporadic or seasonal reintroduction from deeper waters by mixing via upwelling or storms, from organic matter remineralization and from land-based sources (1–3). N stimulates phytoplankton growth, and the connection of N metabolism to photosynthesis has long been recognized (1, 6). The ability to assimilate N from nitrate, ammonium, urea, or guanine dissolved in seawater, or, alternatively, from particulate N sources, and to rapidly sequester N as crystalline guanine for redeployment under conditions of N limitation has emerged as an important survival strategy of free-living phytoplankton algae. N storage is also a critical component of cnidarian-dinoflagellate symbiosis. Natural or anthropogenic N eutrophication is known to disrupt the N-limited state of coral symbionts, disturbing the host's control over them thereby exacerbating the damage following mass coral bleaching (5, 19). By locking excessive N in insoluble crystals and mobilizing them when required, symbiotic microalgae may effectively mitigate the negative effect of N excesses or deprivations and maintain stable nutrient stoichiometry (C:N and N:P ratios). Given the major nutritional role of the symbionts to corals and many other reef animals and the dependence of the reef ecosystem's health on efficient nutrient uptake and storage, our research addressed a critical knowledge gap regarding the mechanisms by which corals acquire and store inorganic nutrients. Such knowledge is increasingly important under escalating eutrophication and climate-induced warming of marine and freshwater ecosystems.

N storage and other diverse vital biological and biochemical functions underscore the versatility of crystalline guanine concerning symbiosis and phytoplankton dynamics. Its shared occurrence among microalgal species over the phylogenetic tree suggests the involvement of guanine in these roles early in evolution, a hypothesis consistent with the potential role of this purine close to the origins of life and its presumably prebiotic occurrence on early Earth (39). Analogous to polyphosphate, which was regarded as a molecular fossil (40) and was, subsequently, revealed to have a multitude of functions (41), the crystalline guanine can also be considered as an evolutionary old, overlooked, and forgotten multifunctional tool of nature popping up from oblivion.

Materials and Methods

Chemicals and Media. References for chemicals and protocols used for preparing cultivation media and stable isotope labeling are listed or described in detail in *SI Appendix*, section II.

Algal Strains, Corals, and Cultivation Protocols. The origins and cultivation conditions for the microalgal species in Table 1 are listed in *SI Appendix*, sections I.4. and II.3. Cnidarian species anemone, *Aiptasia* sp., corallimorpharian, *R. indosinensis*, scleractinian coral, *E. paraancora*, leather coral, *S. asterolobata*, and anthozoan *Zoanthus* sp., were purchased from a local marine aquarium shop. *A. millepora* was collected from the GBR, Australia, and studied immediately after collection or as explants cultivated in experimental aquaria. Details of the laboratory cultivation and methods to study the kinetics of guanine assimilation and turnover are provided in *SI Appendix*, sections I, II.1.A, II.3, and II.4.

Confocal Raman Microscopy. The samples for Raman measurements were prepared and treated according to the methodology described in detail elsewhere (23, 42, 43) and summarized in *SI Appendix*, section II.1.C. The inverted Raman microscope LabRam Evolution (Horiba Scientific, Longjumeau, France) and upright Raman microscope WITec alpha 300 RSA (WITec, Ulm, Germany) were used with laser excitation at 532 nm in the study. To remove interference by autofluorescence of chlorophyll, wide-area low-power photobleaching of entire cells using a defocused 532-nm laser beam was employed before mapping. No differences that would affect data interpretation were observed between measurements on the Horiba and WITec systems.

Confocal Reflection Microscopy. *Symbiodiniaceae* cells of *A. carterae* and *Zoanthus* sp. confirmed by Raman microscopy to include guanine crystals were concurrently imaged using a confocal fluorescence microscope Leica TCS SP8 (Leica Microsystems, Germany) in the reflection mode using laser excitation at 488 nm. The guanine inclusions were seen in the reflection as crystal-like highly light-scattering objects. Further details are provided in *SI Appendix*, sections I.6, II.1.C, and II.4.

Analytical Electron Microscopy. The protocol of specimen preparation for TEM is described in *SI Appendix*, section II.1.E. Ultrathin sections were cut with a LKB-8800 (LKB, Sweden) ultratome, stained with lead citrate according to the method described by Reynolds (44) and examined under a JEM-1011 (JEOL, Tokyo, Japan) electron microscope. Samples for nanoscale elemental analysis using analytical TEM with EDX were fixed, dehydrated, and embedded as above, except that sections were stained with uranyl acetate and lead citrate. Semithin sections were examined under a JEM-2100 (JEOL, Japan) electron microscope. Point EDX spectra were recorded using a JEOL bright-field STEM module and an X-Max X-ray detector system (Oxford Instruments, United Kingdom). Further details are provided in *SI Appendix*, sections II.1.E and II.1.F.

Data Availability. All study data are included in the article and supporting information.

ACKNOWLEDGMENTS. This study received financial support from the Czech Science Foundation (Grant 17-06264S), Russian Science Foundation

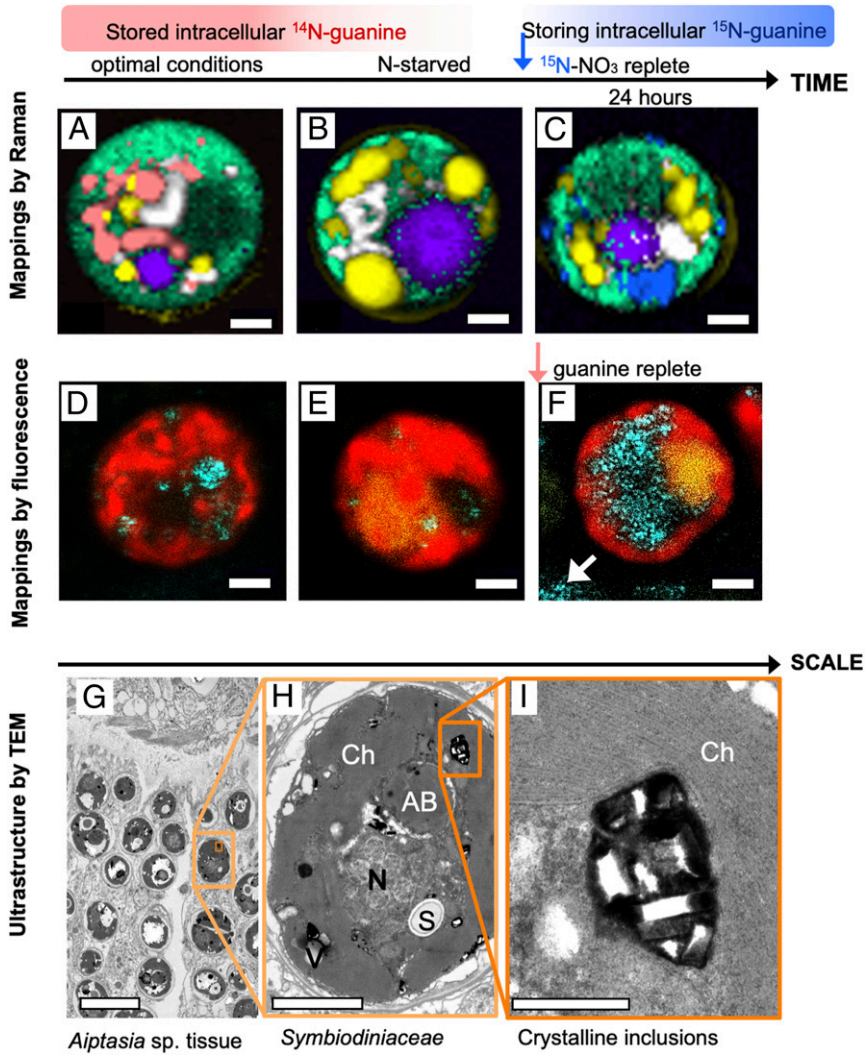

Fig. 7. Guanine in the endosymbiotic *Symbiodiniaceae* cells in corals. Raman maps of cells from tissue of the coral *E. paraancora* (*A*–*C*). The spectra used to construct these maps are shown in *SI Appendix*, Fig. S13. Symbionts in corals maintained under optimal nutrient conditions contained guanine crystals (*A*). Cells from corals that were kept in N-depleted seawater for 4 mo contained very few guanine crystals (*B*). Twenty-four hours after feeding the starved coral 0.3-mM ^{15}N-$NaNO_3$, cells showed large ^{15}N-guanine depots (*C*). The false color coding is the same as that in Figs. 1 and 4 with magenta added to represent accumulation bodies. (Scale bar, 2 μm.) *Symbiodiniaceae* cells isolated from the Great Barrier Reef (GBR) coral, *A. millepora* (*D*–*F*). Cell from freshly collected coral (*D*), N-depleted coral (*E*), and from one day after feeding with medium containing traces of undissolved guanine grains (*F*). Cyan, 488-nm laser reflection of guanine grains outside (white arrow) and inside the cells; red, chlorophyll autofluorescence at 670–700 nm; yellow, fluorescence in accumulation bodies at 500–560 nm; white arrow, remains of undissolved crystalline guanine in medium. (Scale bar, 2 μm.) Ultrastructure of *Symbiodiniaceae* cells in *Aiptasia sp.* shown at increasing magnification (*G*–*I*). AB, accumulation body; Ch, chloroplast; N, nucleus; S, floridean starch; V, vacuole. (Scale bars, 10 [*G*], 2 [*H*], and 0.5 μm [*I*].)

(Grant 20-64-46018), Grant Agency of Charles University (Grant 796217), and the project Algnutrient-UrBioSol (Grant FKZ 031B0453A) of the Federal Ministry of Education and Research, Germany. Electron microscopy was supported by the User Facilities Center of M. V. Lomonosov Moscow State University. Confocal imaging was supported by Western Sydney University.

1. N. J. Antia, P. J. Harrison, L. Oliveira, The role of dissolved organic nitrogen in phytoplankton nutrition, cell biology and ecology. *Phycologia* **30**, 1–89 (1991).
2. P. G. Falkowski, Evolution of the nitrogen cycle and its influence on the biological sequestration of CO_2 in the ocean. *Nature* **387**, 272–275 (1997).
3. P. G. Falkowski, R. T. Barber, V. Smetacek, Biogeochemical controls and feedbacks on ocean primary production. *Science* **281**, 200–207 (1998).
4. D. M. Anderson, P. M. Glibert, J. M. Burkholder, Harmful algal blooms and eutrophication: Nutrient sources, composition, and consequences. *Estuaries* **25**, 704–726 (2002).
5. N. Rädecker, C. Pogoreutz, C. R. Voolstra, J. Wiedenmann, C. Wild, Nitrogen cycling in corals: The key to understanding holobiont functioning? *Trends Microbiol.* **23**, 490–497 (2015).
6. T. Tyrrell, The relative influences of nitrogen and phosphorus on oceanic primary production. *Nature* **400**, 525–531 (1999).
7. S. Schmollinger *et al.*, Nitrogen-sparing mechanisms in *Chlamydomonas* affect the transcriptome, the proteome, and photosynthetic metabolism. *Plant Cell* **26**, 1410–1435 (2014).
8. K. Forchhammer, R. Schwarz, Nitrogen chlorosis in unicellular cyanobacteria–A developmental program for surviving nitrogen deprivation. *Environ. Microbiol.* **21**, 1173–1184 (2019).
9. B. Watzer, K. Forchhammer, Cyanophycin synthesis optimizes nitrogen utilization in the unicellular cyanobacterium *Synechocystis* sp strain PCC 6803. *Appl. Environ. Microbiol.* **84**, e01298-18 (2018).
10. O. Baulina *et al.*, Diversity of the nitrogen starvation responses in subarctic *Desmodesmus* sp. (Chlorophyceae) strains isolated from symbioses with invertebrates. *FEMS Microbiol. Ecol.* **92**, fiw031 (2016).
11. J. Lewis, P. Burton, A study of newly excysted cells of *Gonyaulax polyedra* (Dinophyceae) by electron microscopy. *Br. Phycol. J.* **23**, 49–60 (1988).
12. A. Jantschke *et al.*, Anhydrous β-guanine crystals in a marine dinoflagellate: Structure and suggested function. *J. Struct. Biol.* **207**, 12–20 (2019).
13. R. DeSa, J. W. Hastings, The characterization of scintillons. Bioluminescent particles from the marine dinoflagellate, *Gonyaulax polyedra*. *J. Gen. Physiol.* **51**, 105–122 (1968).

14. K. B. Strychar, P. W. Sammarco, T. J. Piva, Apoptotic and necrotic stages of *Symbiodinium* (Dinophyceae) cell death activity: Bleaching of soft and scleractinian corals. *Phycologia* **43**, 768–777 (2004).
15. D. L. Taylor, *In situ* studies on cytochemistry and ultrastructure of a symbiotic marine dinoflagellate. *J. Mar. Biol. Assoc. U. K.* **48**, 349–366 (1968).
16. M. J. Kevin, W. T. Hall, J. J. McLaughlin, P. A. Zahl, *Symbiodinium microadriaticum* Freudenthal, a revised taxonomic description, ultrastructure. *J. Phycol.* **5**, 341–350 (1969).
17. P. L. Clode, M. Saunders, G. Maker, M. Ludwig, C. A. Atkins, Uric acid deposits in symbiotic marine algae. *Plant Cell Environ.* **32**, 170–177 (2009).
18. T. Krueger *et al*., Temperature and feeding induce tissue level changes in autotrophic and heterotrophic nutrient allocation in the coral symbiosis–A NanoSIMS study. *Sci. Rep.* **8**, 12710 (2018).
19. S. Rosset, J. Wiedenmann, A. J. Reed, C. D'Angelo, Phosphate deficiency promotes coral bleaching and is reflected by the ultrastructure of symbiotic dinoflagellates. *Mar. Pollut. Bull.* **118**, 180–187 (2017).
20. H. Yamashita, A. Kobiyama, K. Koike, Do uric acid deposits in *zooxanthellae* function as eye-spots? *PLoS One* **4**, e6303 (2009).
21. C. Kopp *et al*., Highly dynamic cellular-level response of symbiotic coral to a sudden increase in environmental nitrogen. *MBio* **4**, e00052–e13 (2013).
22. A. Jantschke, I. Pinkas, A. Schertel, L. Addadi, S. Weiner, Biomineralization pathways in calcifying dinoflagellates: Uptake, storage in MgCaP-rich bodies and formation of the shell. *Acta Biomater.* **102**, 427–439 (2020).
23. Š. Moudříková, L. Nedbal, A. Solovchenko, P. Mojzeš, Raman microscopy shows that nitrogen-rich cellular inclusions in microalgae are microcrystalline guanine. *Algal Res.* **23**, 216–222 (2017).
24. D. Gur, B. A. Palmer, S. Weiner, L. Addadi, Light manipulation by guanine crystals in organisms: Biogenic scatterers, mirrors, multilayer reflectors and photonic crystals. *Adv. Funct. Mater.* **27**, 1603514 (2017).
25. S. Menden-Deuer, E. J. Lessard, Carbon to volume relationships for dinoflagellates, diatoms, and other protist plankton. *Limnol. Oceanogr.* **45**, 569–579 (2000).
26. A. Shebanova *et al*., Versatility of the green microalga cell vacuole function as revealed by analytical transmission electron microscopy. *Protoplasma* **254**, 1323–1340 (2017).
27. T. Ismagulova, A. Shebanova, O. Gorelova, O. Baulina, A. Solovchenko, A new simple method for quantification and locating P and N reserves in microalgal cells based on energy-filtered transmission electron microscopy (EFTEM) elemental maps. *PLoS One* **13**, e0208830 (2018).
28. R. E. Schmitter, The fine structure of *Gonyaulax polyedra*, a bioluminescent marine dinoflagellate. *J. Cell Sci.* **9**, 147–173 (1971).
29. J. D. Dodge, Ultrastructure of dinoflagellate pusule - unique osmo-regulatory organelle. *Protoplasma* **75**, 285–302 (1972).
30. R. Onuma, T. Horiguchi, Morphological transition in kleptochloroplasts after ingestion in the dinoflagellates *Amphidinium poecilochroum* and *Gymnodinium aeruginosum* (Dinophyceae). *Protist* **164**, 622–642 (2013).
31. D. Gur *et al*., Guanine crystallization in aqueous solutions enables control over crystal size and polymorphism. *Cryst. Growth Des.* **16**, 4975–4980 (2016).
32. H. J. Jeong *et al*., Heterotrophic feeding as a newly identified survival strategy of the dinoflagellate *Symbiodinium*. *Proc. Natl. Acad. Sci. U.S.A.* **109**, 12604–12609 (2012).
33. J. M. Delabar, M. Majoube, Infrared and Raman-spectroscopic study of N-15 and D-substituted guanines. *Spectrochim. Acta A* **34**, 129–140 (1978).
34. L. Muscatine, J. W. Porter, Reef corals: Mutualistic symbioses adapted to nutrient-poor environments. *BioSci.* **27**, 454–460 (1977).
35. D. Yellowlees, T. A. V. Rees, W. Leggat, Metabolic interactions between algal symbionts and invertebrate hosts. *Plant Cell Environ.* **31**, 679–694 (2008).
36. K. L. Barott, A. A. Venn, S. O. Perez, S. Tambutté, M. Tresguerres, Coral host cells acidify symbiotic algal microenvironment to promote photosynthesis. *Proc. Natl. Acad. Sci. U.S.A.* **112**, 607–612 (2015).
37. P. G. Falkowski, The role of phytoplankton photosynthesis in global biogeochemical cycles. *Photosynth. Res.* **39**, 235–258 (1994).
38. A. Hirsch *et al*., "Guanigma": The revised structure of biogenic anhydrous guanine. *Chem. Mater.* **27**, 8289–8297 (2015).
39. N. Kitadai, S. Maruyama, Origins of building blocks of life: A review. *Geoscience Frontiers* **9**, 1117–1153 (2018).
40. A. Kornberg, N. N. Rao, D. Ault-Riché, Inorganic polyphosphate: A molecule of many functions. *Annu. Rev. Biochem.* **68**, 89–125 (1999).
41. L. Xie, U. Jakob, Inorganic polyphosphate, a multifunctional polyanionic protein scaffold. *J. Biol. Chem.* **294**, 2180–2190 (2019).
42. Š. Moudříková *et al*., Raman and fluorescence microscopy sensing energy-transducing and energy-storing structures in microalgae. *Algal Res.* **16**, 224–232 (2016).
43. Š. Moudříková *et al*., Quantification of polyphosphate in microalgae by Raman microscopy and by a reference enzymatic assay. *Anal. Chem.* **89**, 12006–12013 (2017).
44. E. S. Reynolds, The use of lead citrate at high pH as an electron-opaque stain in electron microscopy. *J. Cell Biol.* **17**, 208–212 (1963).